Thermochimica Acta 653 (2017) 49–58

Contents lists available at ScienceDirect

Thermochimica Acta

journal homepage: www.elsevier.com/locate/tca

Effects of SiO_2 nanoparticles on structure and property of form-stable phase change materials made of cellulose acetate phase inversion membrane absorbed with capric-myristic-stearic acid ternary eutectic mixture

Yibing Cai[a,*], Xuebin Hou[a], Weiwei Wang[a], Mengmeng Liu[a], Junhao Zhang[b], Hui Qiao[a], Fenglin Huang[a], Qufu Wei[a,*]

[a] Key Laboratory of Eco-Textiles, Ministry of Education, Jiangnan University, Wuxi, Jiangsu 214122, China
[b] School of Environmental and Chemical Engineering, Jiangsu University of Science and Technology, Zhenjiang, Jiangsu 212003, China

ARTICLE INFO

Keywords:
Cellulose acetate (CA) phase inversion membrane
SiO_2 nanoparticles
Capric-myristic-stearic acid (CMS) ternary eutectic mixture
Form-stable phase change materials (PCMs)

ABSTRACT

The innovative form-stable phase change materials (PCMs) were fabricated by incorporating capric-myristic-stearic acid (CMS) ternary eutectic mixture with cellulose acetate (CA) phase inversion membrane. CMS as model PCM, with melting point near ambient temperature as the temperature range was most valuable in practice. Effects of different SiO_2 amounts on surface features, structural morphology and absorption capacity of CA membrane were investigated. The SiO_2 nanoparticles created porous structure and increased CMS incorporation capability of CA membrane, the maximum absorption capacity of CA-SiO_2 membrane was ~80.3 wt.%. The enthalpies of melting of form-stable PCMs were 76.6 kJ/kg for CA membrane and 99.8 kJ/kg for CA-SiO_2 membrane, respectively. The SiO_2 nanoparticles increased remarkably thermal stability property of form-stable PCMs. As compared to CA-SiO_2 membrane, the control temperature time of CMS/CA-SiO_2 form-stable PCMs was increased by ~46.8%. The developed form-stable PCMs demonstrated good thermal storage/retrieval property and thermal insulation capability.

1. Introduction

The mismatch between energy supply and demand during energy conversion and delivery is a critical problem in the numerous applications such as building heating/cooling systems, the utilization of solar energy, industrial waste heat recovery and air-conditioning systems, *etc* [1–5]. Thermal energy storage can solve the problem and significantly increase the efficiency of systems; among various methods for the storage of thermal energy, the storage and retrieval of thermal energy by using phase change materials (PCMs) have attracted extensive attentions due to their high energy storage capacity and small temperature variation during phase transition process [6–8].

Among the large number of PCMs, fatty acids and/or their eutectics have been extensively studied as a promising type of solid-liquid PCMs due to their superior properties such as appropriate melting temperature range, high heat storage capacity, little or no super-cooling, low vapor pressure, non-toxicity, non-corrosiveness, and good chemical/thermal stability [9–13]. However, fatty acids and/or their eutectics have to be placed in specially designed devices/containers in practical application to prevent the leakage during solid-liquid phase transition process. Such a situation not only raises thermal resistance, but also increases the operational costs. To solve this problem, Form-stable (or shape-stabilized) PCMs have become a research hotspot in thermal energy storage/retrieval field; because they possess the advantageous properties including no need for additional encapsulation, cost-effectiveness, stable shape, and easily fabrication for applications with preferred sizes/dimensions [14–35].

The so-called form-stable PCMs are actually composite materials consisting of PCMs (to store and release thermal energy) and supporting materials (to maintain the solid shape of form-stable PCMs). There are various methods to fabricate form-stable PCMs: (1) encapsulating or microencapsulating PCMs (*e.g.*, fatty acids and/or their eutectics) into polymeric structure by self-polymerization, *in-situ* polymerization and solution casting method [17,18]. (2) Encapsulating PCMs into three-dimensional network *via* sol-gel method [19,20]. (3) Absorbing PCMs into porous materials like expanded graphite [21–25], diatomite [26–28], carbon nanospheres [29], attapulgite [30,31], expanded perlite [32–35] and vermiculite [36,37]. (4) Stable PCM fibrous mats by electrospinning composite spin dope containing both PCMs and polymer matrix [38–41]. Among various fabricated methods, direct

* Corresponding authors.
E-mail addresses: yibingcai@jiangnan.edu.cn (Y. Cai), qfwei@jiangnan.edu.cn (Q. Wei).

http://dx.doi.org/10.1016/j.tca.2017.03.027
Received 20 December 2016; Received in revised form 8 March 2017; Accepted 30 March 2017
Available online 01 April 2017

incorporation of molten PCMs into porous matrix is a quite straightforward method to obtain form-stable PCMs. It is well known that overlaid nanofibrous mat is an excellent candidate to incorporate substantial amount of fatty acid and/or their eutectics for form-stable PCMs. In our previous research, fatty acids and/or their eutectics were successfully absorbed in and then supported by electrospun nanofibrous mats including polyamide 6 [41,42], polyacrylonitrile and its derived carbon [43], SiO_2 [44,45] and cellulose acetate [46]. Although these methods for form-stable PCMs have successfully prevented the leakage of fatty acids and/or their eutectics, the application range is still restricted due to some drawbacks: (1) the preparation process is complex and will increase cost, (2) the efficiency of thermal energy storage is still low by introducing of large amount of supporting materials, (3) the resultant form-stable PCMs have not tunable dimensions/sizes.

The phase inversion membrane induced by immersion precipitation technique possess excellent properties including excellent toughness, high biocompatibility, high selectivity, simple making process, good film-forming performance and low cost [47,48]. The porosities of phase inversion membrane can be exceptionally high; hence, they have the potential to be utilized as the supporting materials for the preparation of form-stable PCMs. However, to the best of our knowledge, the investigations on form-stable PCMs with fatty acid and/or their eutectics being encapsulated in and/or supported by phase inversion membrane through physical absorption have not been reported. Therefore, in this study, cellulose acetate (CA) phase inversion membrane was firstly prepared and chosen as supporting materials. The motivation of SiO_2 nanoparticles addition was further to create surface porous structure and specific surface area of phase inversion membrane, and then increased incorporation capability of CA phase inversion membrane [49–51]. Subsequently, capric-myristic-stearic acid (CMS) ternary eutectic mixture was prepared as a model PCM followed by being absorbed in and supported by CA and/or CA-SiO_2 phase inversion membrane to fabricate form-stable PCMs. Morphological structures, CMS absorption capacity, thermal energy storage property, as well as thermal insulation property of the resultant form-stable PCMs were investigated. The fabricated form-stable PCMs demonstrated good thermal storage/retrieval capability and great temperature regulation ability. It is envisioned that this innovative type of form-stable PCMs play an important role in the potential applications of temperature-regulating textiles and building energy efficiency (*e.g.*, wallboards/concretes, roofs and/or floor boards).

2. Experimental

2.1. Materials

The powders of cellulose acetate (CA, M_n = 29,000 g/mol), capric acid (CA), myristic acid (MA) and stearic acid (SA), the SiO_2 nanoparticles (white powder, with average particle size of ~15 nm), acetone and *N*,*N*-dimethylacetamide (DMAc), were supplied by the Shanghai Chemical Regents Co. (Shanghai, China). All of the chemicals/materials were used without further purification.

2.2. Preparation of CMS ternary eutectic mixture

Capric-myristic-stearic acid (CMS) ternary eutectic mixture was prepared using theoretical calculation and experimental procedure in literature [11–16]. Mass ratio of CA, MA and SA in the eutectic mixture was determined as 76.97:18.55:4.48. The CMS mixture was heated to 80 °C for 2 h until completely molten, and then magnetically stirred for 2 min to ensure homogeneity. Subsequently the CMS mixture was cooled down to room temperature in air to get it ready for PCM use. Thermal properties of individual fatty acids (*i.e.*, CA, MA and SA) and CMS ternary eutectic mixture were acquired from differential scanning calorimetry (DSC) measurements, and the DSC curves and thermal characteristics are shown in Fig. 1 and Table 1.

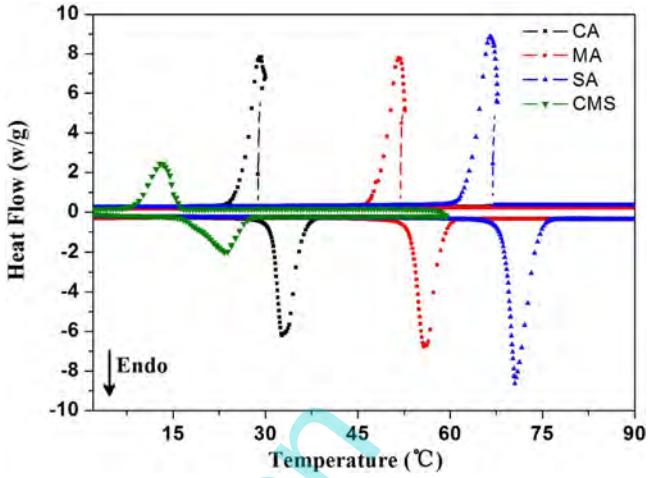

Fig. 1. DSC curves of individual fatty acids (*i.e.*, CA, MA and SA) and CMS ternary eutectic mixture.

Table 1
The extrapolated peak onset temperatures (T_e), melting peak temperature (T_m), crystallization peak temperature (T_c), melting enthalpy (ΔH_m) and crystallization enthalpy (ΔH_c) of CA, MA, SA and CMS ternary eutectic mixture.

Samples	Heating process			Cooling process		
	T_e (°C)	T_m (°C)	ΔH_m (kJ/kg)	T_e (°C)	T_c (°C)	ΔH_c (kJ/kg)
CA	31.1	32.7	166.7	29.3	29.2	163.1
MA	53.7	56.1	187.3	52.1	51.9	184.9
SA	69.0	70.5	222.8	67.1	66.5	226.7
CMS	17.4	23.6	122.8	15.3	13.1	119.7

2.3. Preparation of CA and CA-SiO_2 phase inversion membranes

The immersion precipitation phase transformation technique was utilized to prepare CA phase inversion membrane. The powders of CA (10 wt.%) was firstly dissolved in mixture solvents with the mass ratio of acetone/DMAc being 2/1, then varied mass fractions (*i.e.,* 5%, 7.5%, 10%, 12.5% and 15 %) of SiO_2 nanoparticles were added into CA solutions followed by magnetic stirring for 12 h and ultrasonication for 60 min to achieve the homogeneous dispersion. The motivation for the addition of SiO_2 nanoparticles was to increase the specific surface area as well as the porous structure of CA phase inversion membrane [49–51]. Prior to the preparation of mixture solutions, the SiO_2 nanoparticles were desiccated under vacuum at 80 °C.

Subsequently, the mixture solutions were hold for 4 h at room temperature without stirring to complete removal of air bubbles. The casting solutions were casted onto glass plate through thin film applicator (K202 Control Coater-Model) with adjusting thickness of 250 μm. Then glass plate coated by casted membranes were immediately immersed in distilled water for 10 min. The casted membranes were washed three times and dried under vacuum at 60 °C for 10 h to remove residual solvents and were termed as CA-1, CA-2, CA-3, CA-4 and CA-5, respectively. The schematic illustration for preparation of CA and CA-SiO_2 phase inversion membranes was shown in Fig. 2.

2.4. Fabrication of form-stable PCMs

The prepared CMS ternary eutectic mixture was firstly placed in a beaker at 60 °C until being melted completely. Then, CA and CA-SiO_2 phase inversion membranes were immersed into molten CMS ternary eutectic mixture for 60 min to ensure saturate absorption. The phase inversion membranes with absorbed CMS ternary eutectic mixture were finally hung in an oven at 60 °C for 10 h to remove excess CMS on surface of phase inversion membranes.

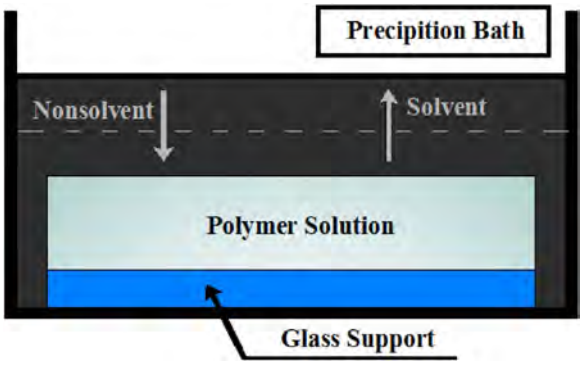

Fig. 2. Schematic illustration for preparation of CA and CA-SiO_2 phase inversion membranes.

2.5. Characterization

Scanning electron microscopy (SEM, SU1510) was employed to examine the surface and cross-section morphologies of CA and CA-SiO_2 phase inversion membranes and resultant form-stable PCMs. Before SEM examination, all specimens were sputter-coated with gold to avoid charge accumulations. A CSPM-4000 atomic force microscopy (AFM) was used to observe surface morphology and roughness of resultant form-stable PCMs and the corresponding CA and CA-SiO_2 phase inversion membranes. Scanning was carried out in tapping mode. All images were obtained at ambient conditions.

The Brunauer–Emmett–Teller (BET) method was adopted to determine the specific surface area of CA and CA-SiO_2 phase inversion membranes. The desorption data of N_2 isotherm were analyzed by the Barrett–Joyner–Halenda (BJH) method to acquire the value of specific surface area. The BET specific surface area for each sample was measured for 3 times, and the average value was reported.

Thermal energy storage/retrieval properties of CA, MA, SA, CMS ternary eutectic mixture and resultant form-stable PCMs were carried out using a DSC Q200 thermal analyzer. The flow rate of N_2 was set at 25 ml/min, and DSC curves were recorded from 0 to 50 °C with the scanning rate of 5 °C/min. The precisions of measurements for calorimeter and temperature was ± 2.0% and ± 2.0 °C, respectively. The enthalpies of melting (ΔH_m) and crystallization (ΔH_c) of individual fatty acids and CMS ternary eutectic mixture were calculated based upon areas under the melting/crystallization DSC peaks through the thermal analysis software affiliated with the equipment.

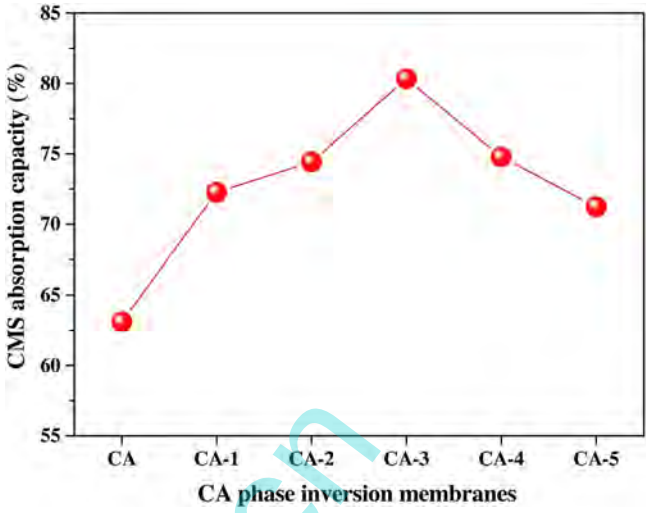

Fig. 4. CMS absorption capacities of CA and CA-SiO_2 phase inversion membranes.

Thermogravimetric analyses were conducted by using a TGA-Q500 thermo-analyzer instrument; the heating rate was set at 10 °C/min, and the TGA curves were recorded from 20 to 700 °C under 40 ml/min flow of nitrogen. The amounts of samples for the TGA analyses were ~10 mg. The precisions of measurements for temperature and mass during TGA experiments were ± 2.0 °C and ± 2.0%, respectively.

The thermal insulation capability of fabricated form-stable PCMs was evaluated and compared with non-PCM containing phase inversion membranes by using a self-assembled control temperature measurement, as shown in Fig. 3. The designed heating setup mainly consisted of a foam-box (150 × 150 × 150 mm^3) with a 100 W lamp served as thermal radiation source and mounted at the top. And test setup also consisted of the same size foam-box with a thermocouple inside. The heating setup and test setup were separated by a foam board. A cavity in central position of the foam board surface was made for placing sample with the size of 80 × 100 × 2 mm^3. The lamp of heating setup began to heating until the indoor air temperature of test setup reached to 50 °C, then the air temperature variations in the test setup were monitored and automatically recorded by a computer. The recorded temperature range was from initial temperature of 50 °C to the balanced temperature of 19 °C for each sample. The measurement of

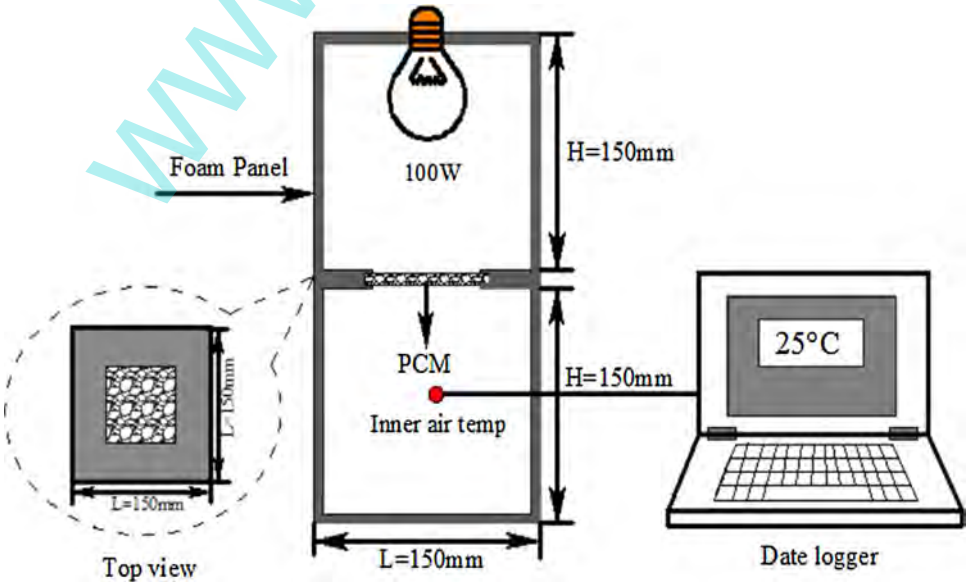

Fig. 3. Schematic illustration of thermal insulation test setup for form-stable PCMs.

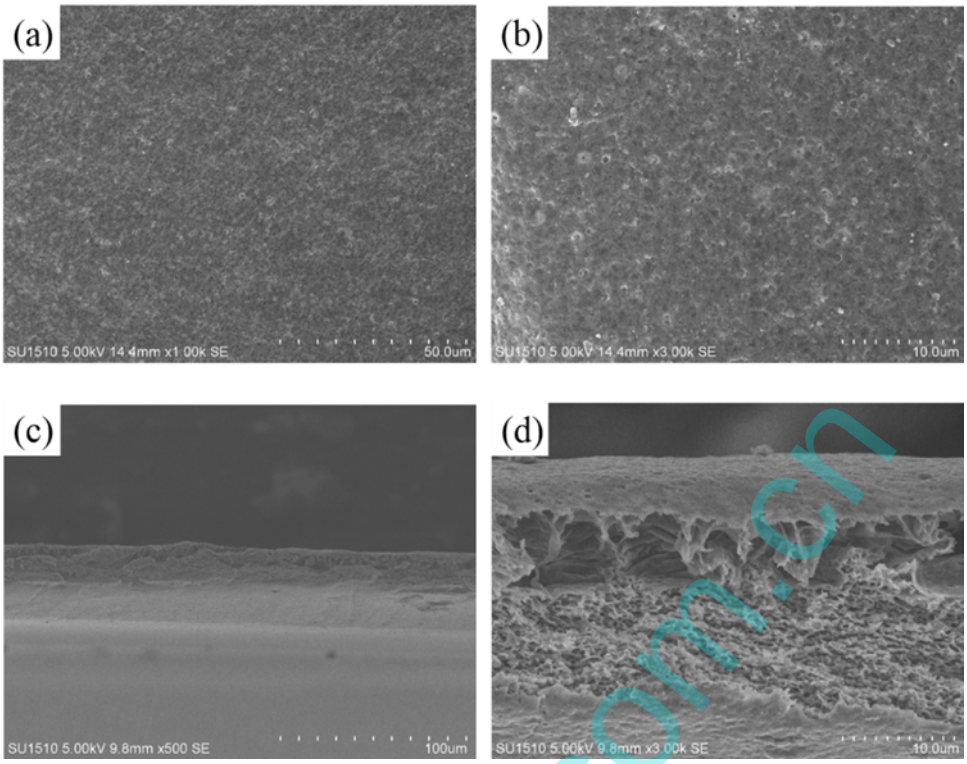

Fig. 5. SEM images of CA phase inversion membrane: (a, b) surface morphology, and (c, d) cross-section.

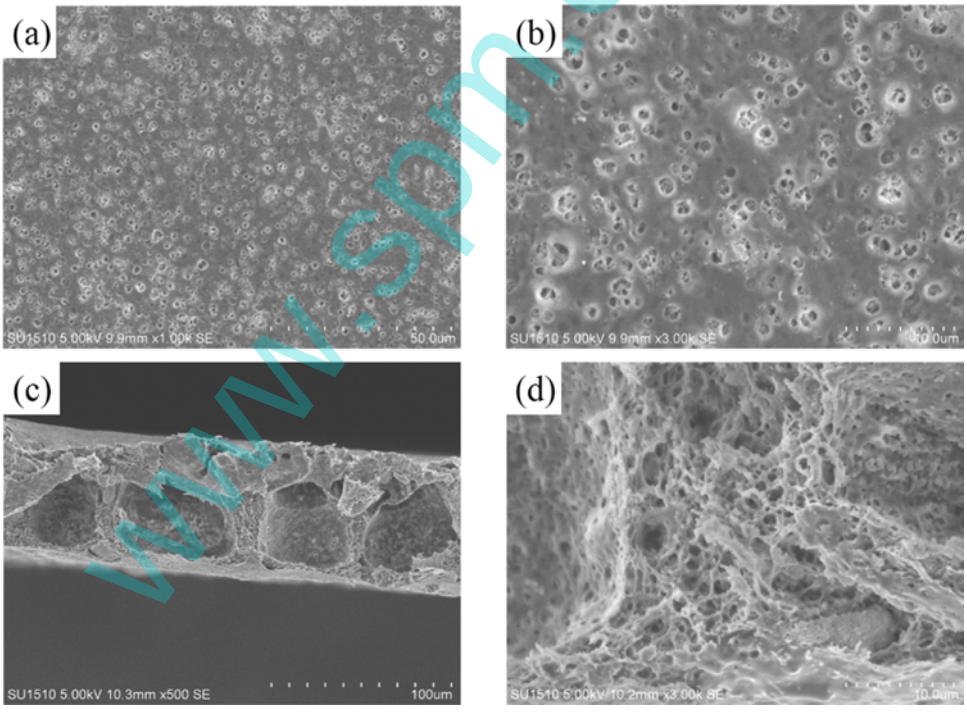

Fig. 6. SEM images of CA-SiO_2 phase inversion membrane: (a, b) surface morphology, and (c, d) cross-section.

each sample was repeated for 3 times, and the average value was reported in this study.

3. Results and discussion

3.1. Absorption capacity of CA phase inversion membranes

The absorption capacity of CMS ternary eutectic mixture in phase inversion membranes directly determines thermal energy storage/retrieval and temperature regulation properties of fabricated form-stable PCMs. CMS absorption capacity of phase inversion membranes can be calculated using the following equation:

$$\text{Absorption capacity} = \frac{m - m_0}{m_0} \times 100\%$$

where m_0 and m are the mass of phase inversion membranes before and after the absorption of CMS ternary eutectic mixture, respectively. The

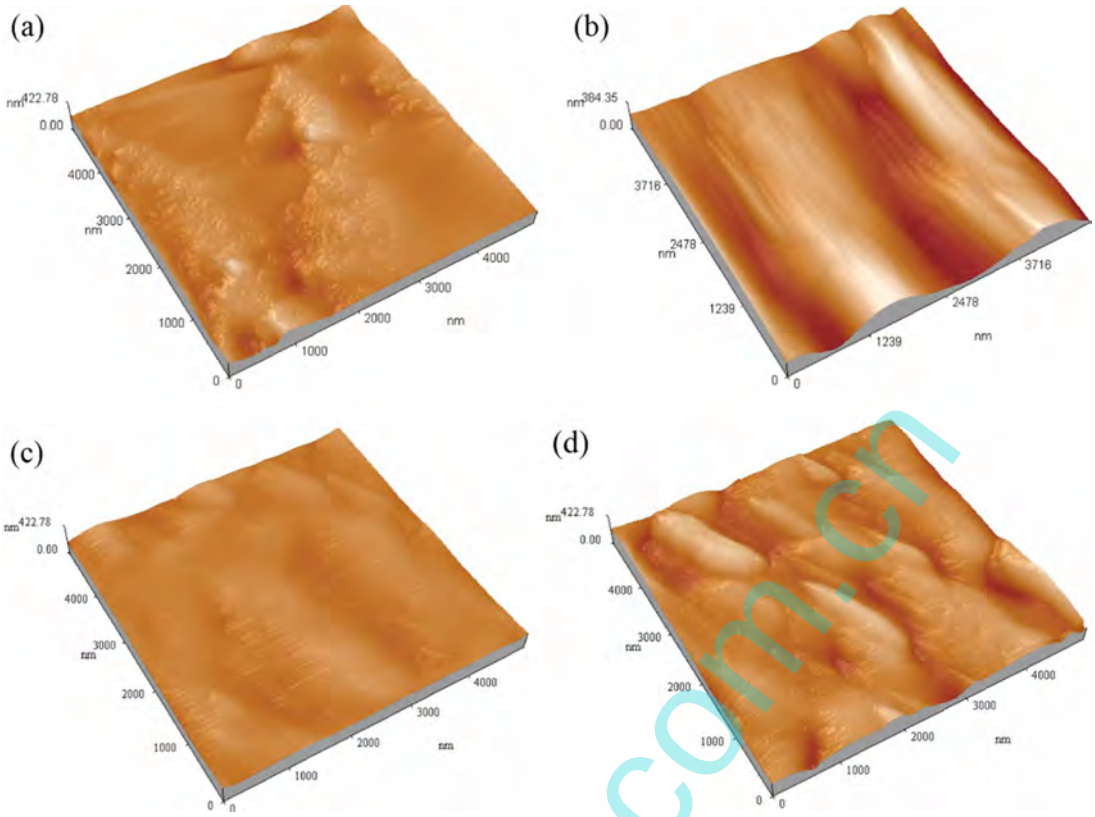

Fig. 7. AFM images of (a) CA and (b) CA-SiO_2 phase inversion membranes; (c) CMS/CA and (d) CMS/CA-SiO_2 form-stable PCMs.

Table 2
Surface roughness parameters of CA and CA-SiO_2 phase inversion membranes before and after absorbing CMS ternary eutectic mixture.

Sample	Sa (nm)	S_q (nm)	S_z (nm)
CA	15.9	21.0	175
CMS/CA	10.4	13.4	83.3
CA-SiO_2	46.6	56.2	294
CMS/CA-SiO_2	26.1	33.1	130

experiments are repeated for three times and the average value is acquired. The results are reproducible with standard deviation typically less than ± 2.0%.

CMS absorption capacities of CA and CA-SiO_2 (with different SiO_2 mass fractions. *i.e.,* 5 %, 7.5 %, 10 %, 12.5% and 15 %) phase inversion membranes were plotted in Fig. 4. The calculated absorption capacities of phase inversion membranes were 63.1% for CA, 72.3% for CA-1, 74.4% for CA-2, 80.3% for CA-3, 74.8% for CA-4 and 71.2% for CA-5, respectively. The result indicated that the phase inversion membranes were in favor of absorbing large amount of CMS ternary eutectic mixture due to their porous structure and high surface-to-volume ratio. The CMS absorption capacities of CA-SiO_2 phase inversion membranes were notably higher than those of CA phase inversion membrane. Such a result might be attributed to enhanced specific surface area as well as the porous structure of phase inversion membrane upon the addition of SiO_2 nanoparticles [49–51], leading to the increase of absorption amount. Meanwhile, excess SiO_2 can be adsorbed and/or deposited on the membrane surface, causing membrane fouling which in turn reduce the porosity drastically. In addition, the decrease in absorption capacity on fatty acid with hydrophobic characteristic was also due to the increase in surface hydrophilicity which was rendered by SiO_2 particles. Similar results were reported for CA/SiO_2 blend membranes [49,52]. Since the CA-3 phase inversion membrane with 10 wt.% SiO_2 mass fraction, showed the higher CMS absorption capacity, hence it was selected to make CMS-based form-stable PCMs in the following research.

3.2. Microstructure and surface morphology of CA phase inversion membranes

The surface and cross-section morphologies of CA and CA-SiO_2 phase inversion membranes are characterized by SEM, and the representative images are shown in Figs. 5 and 6, respectively. It could be seen from Fig. 5(a) and (b) that CA phase inversion membrane had compact structure, there was almost no porous morphology on surface. Similar structural morphology had also been reported in literatures [53,54]. Meanwhile, the cross-section morphology showed that CA phase inversion membrane had relatively irregular structure and had no obvious macroporous structure. The upper layer of membrane appeared discontinuous porous structure, but the lower layer of membrane possessed interconnected and small porous structure, as shown in Fig. 5(c) and (d). Such porous structure was capable of absorbing a large amount of PCMs (*i.e.*, CMS).

On the contrast, the CA-SiO_2 phase inversion membrane had uniform porous structure with pore size of a few microns, and pores of different layers of membranes were mutually staggered, as shown in Fig. 6(a) and (b). It could be also seen from Fig. 6(c) and (d) that the cross-section of CA-SiO_2 phase inversion membrane was interconnected with uniform macropores with pore size of several tens of microns, and the pores were connected with each other and mutual permeable. This demonstrated that the addition of SiO_2 nanoparticles could significantly change the morphological structure of phase inversion membrane, which created porous structure on membrane surface and was helpful to increase incorporation capability of CMS ternary eutectic mixture.

The surface morphology of CA and CA-SiO_2 phase inversion membranes was further investigated by AFM, the representative AFM images are shown in Fig. 7. The surface roughness parameters of the membrane which were expressed in terms of the mean roughness (S_a),

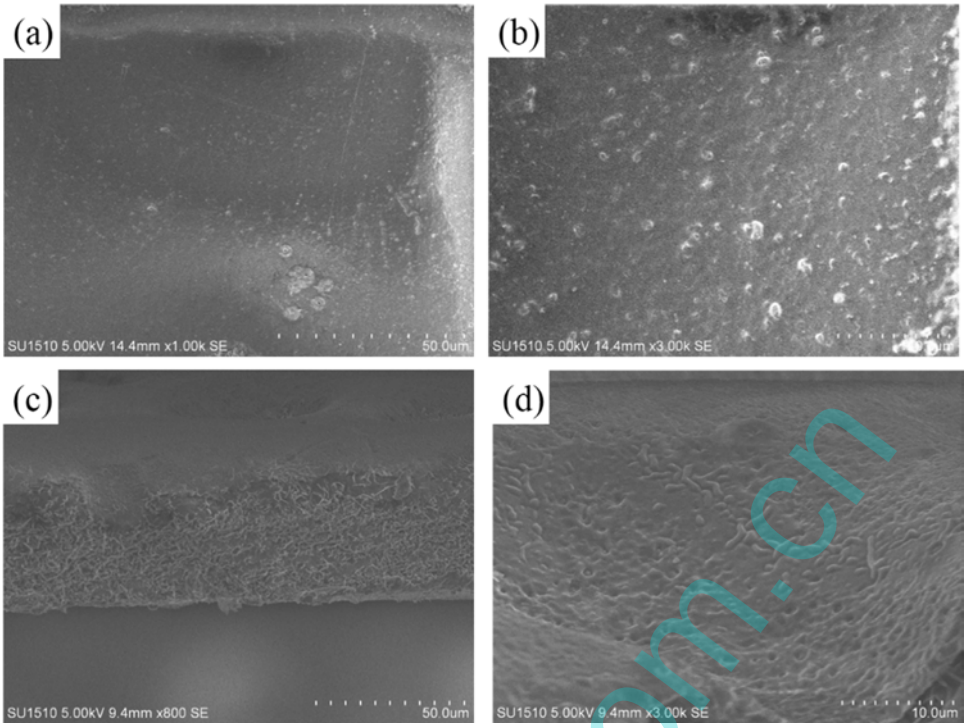

Fig. 8. Representative SEM images of CMS/CA form-stable PCMs: (a, b) surface morphology, and (c, d) cross-section.

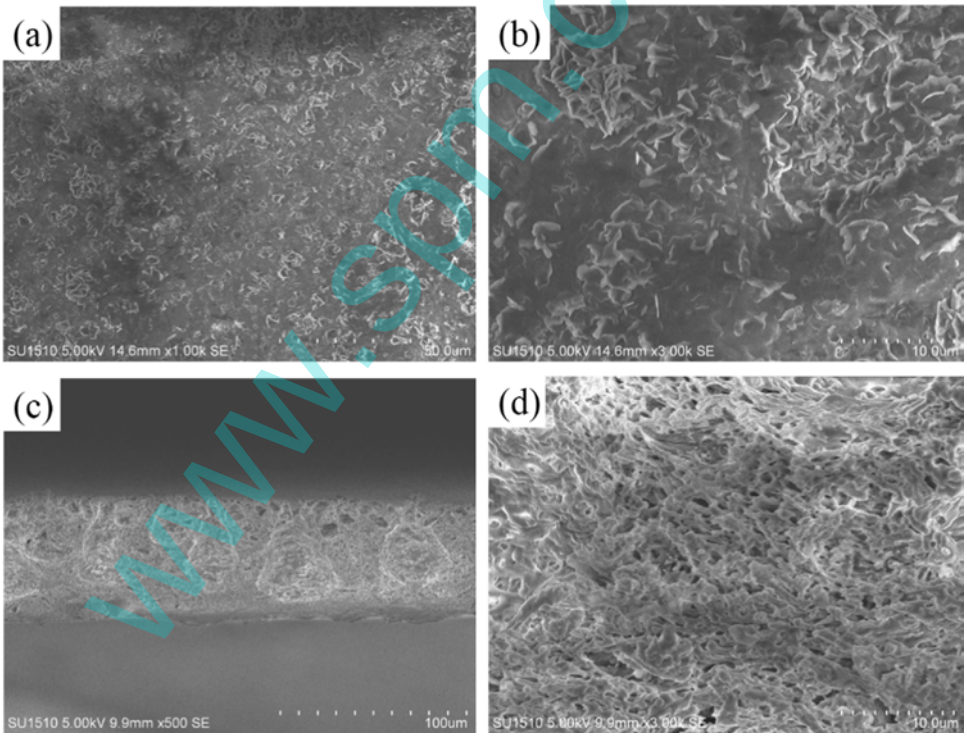

Fig. 9. Representative SEM images of CMS/CA-SiO_2 form-stable PCMs: (a, b) surface morphology, and (c, d) cross-section.

the root mean square of z data (S_q) and the mean difference between the highest peaks and lowest valleys (S_z) were calculated by AFM software in 5 μm × 5 μm scan size (Table 2). The results of Fig. 7 and Table 2 indicated that the CA phase inversion membrane had relatively smooth surfaces with average roughness of ~15.9 nm. However, the CA-SiO_2 phase inversion membrane had rough surfaces with average roughness of ~46.6 nm. Meanwhile, the Brunauer–Emmett–Teller (BET) method was also used to determine the specific surface area of phase inversion membranes. The BET specific surface area of CA and CA-SiO_2 phase inversion membrane was ~16.4 m^2/g and ~18.5 m^2/g, respectively. This indicated that the addition of SiO_2 nanoparticles increased surface roughness and specific surface area of phase inversion membranes, which attributed to high CMS incorporation in the membrane. This result was consistent with the above absorption capacity analysis.

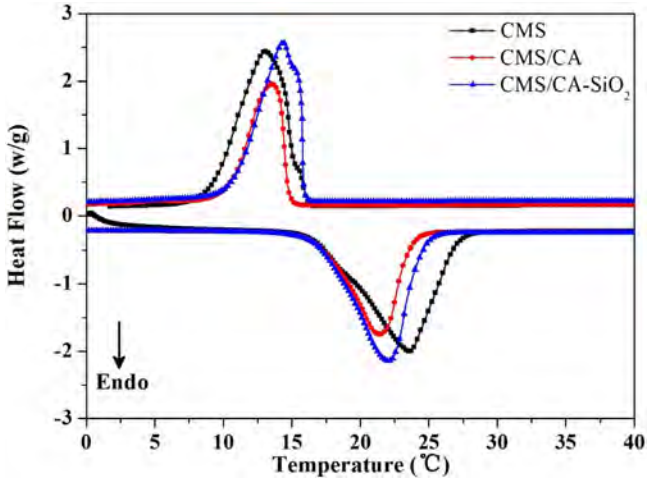

Fig. 10. DSC curves of CMS ternary eutectic mixture, CMS/CA and CMS/CA-SiO_2 form-stable PCMs.

Table 3
Thermal behaviors of CMS ternary eutectic mixture, CMS/CA and CMS/CA-SiO_2 form-stable PCMs.

Samples	Heating process			Cooling process		
	T_e (°C)	T_m (°C)	ΔH_m (kJ/kg)	T_e (°C)	T_c (°C)	ΔH_c (kJ/kg)
CMS	17.4	23.6	122.8	15.3	13.1	119.7
CMS/CA	17.5	21.4	76.6	14.7	13.5	74.7
CMS/CA-SiO_2	17.6	22.0	99.8	15.8	14.4	96.7

Table 4
Comparisons on thermal energy storage properties of some form-stable PCMs.

Form-stable PCMs	T_m (°C)	$\triangle H_m$ (kJ/kg)	T_c (°C)	$\triangle H_c$ (kJ/kg)	Refs
MA-PA-SA (92.86 wt.%)/EG	41.64	153.5	42.99	151.4	[22]
CA-LA-OA (93.7 wt.%)/EG	19.04	109.18	12.19	115.28	[23]
PA-SA (92.9 wt.%)/EG	53.89	166.27	54.37	166.13	[24]
CA-MA-PA (92.9 wt.%)/EG	18.61	128.2	16.58	124.5	[25]
PA-CA (66.6 wt.%)/Diatomite	28.7	104.0	19.7	96.1	[26]
LA (37.5 wt.%)/Diatomite	40.9	57.4	38.7	57.2	[27]
CA-LA (34.0 wt.%)/Diatomite	20.13	66.81	–	–	[28]
SA-CA (50 wt.%)/a-ATP	21.8	72.6	20.3	71.3	[30]
CA-MA (55 wt.%)/EP	21.70	85.40	20.70	89.75	[32]
LA-PA-SA (55 wt.%)/EP	31.8	81.5	30.3	81.3	[33]
LA-SA (43.5 wt.%)/EP	37.6	131.3	–	–	[34]
LA(70 wt.%)/EP	43.2	105.58	–	–	[35]
CA-LA (40 wt.%)/VMT	19.09	61.03	19.15	58.09	[36]
CA-MA (20 wt.%)/VMT	23.35	27.46	14.54	31.42	[37]
CA-LA (90.7 wt%)/PA6/EG	22.28	102.7	16.61	102.2	[41]
CA-LA-PA (81.3 wt.%)/SiO_2 NFs	21.7	100.9	6.4	96.5	[44]
CA-PA (84.2 wt.%)/SiO_2 NFs	28.1	108.6	18.7	102.2	[45]
CMS(80.3 wt.%)/CA-SiO_2	22.0	99.8	14.4	96.7	Present

3.3. Structural morphologies of form-stable PCMs

Structural morphologies of phase inversion membranes absorbed with CMS ternary eutectic mixture were characterized by SEM, and the SEM images of Figs. 8 and 9 were acquired from form-stable PCMs of CMS/CA and CMS/CA-SiO_2, respectively. The Fig. 8(a) and (b) showed the CMS/CA form-stable PCMs had smooth surfaces, and CMS ternary eutectic mixture might partly accumulate on or near the surfaces of phase inversion membranes. In addition, the cross-section pores of CA phase inversion membrane was filled with CMS, leading to unclear interfaces between membrane and CMS ternary eutectic mixture, as shown in Fig. 8(c) and (d). Meanwhile, the results of AFM image (as shown in Fig. 7(c)) and Table 2 also confirmed above deduction. The average roughness of CMS/CA form-stable PCMs was reduced to ~10.4 nm from ~15.9 nm for CA phase inversion membrane.

The images Fig. 9(a) and (b) demonstrated that CMS/CA-SiO_2 form-stable PCMs had relatively coarse surfaces, and the pores on the surface of CA-SiO_2 phase inversion membrane were full of CMS. In addition, the partly aggregation of CMS with lamellar structure could be also observed. Compared to the form-stable PCMs consisting of CA phase inversion membrane, the form-stable PCMs consisting of CA-SiO_2 phase inversion membrane appeared easier to identify worm-like porous structure, which made it to absorb more CMS, as showed in Fig. 9(c) and (d). The average roughness of CMS/CA-SiO_2 form-stable PCMs with ~26.1 nm was higher than that of CMS/CA form-stable PCMs with ~10.4 nm, might be due to the surface lamellar structure on phase inversion membrane, as indicated in Fig. 7(d) and Table 2. It was noteworthy that the porous structure of CA and CA-SiO_2 phase inversion membranes could provide the mechanical support for form-stable PCMs and could effectively prevent the flow/leakage of molten CMS ternary eutectic mixture.

3.4. Thermal energy storage/retrieval properties of form-stable PCMs

Thermal energy storage/retrieval properties of individual fatty acids (*i.e.*, CA, MA, and SA) and the prepared CMS ternary eutectic mixture are characterized by DSC, as shown in Fig. 1. The data of extrapolated peak onset temperatures (T_e), melting peak temperature (T_m), crystallization peak temperature (T_c), melting enthalpy (ΔH_m) and crystallization enthalpy (ΔH_c) are listed in Table 1. The results revealed that prepared CMS ternary mixture presented single endothermic/exothermic peak, indicating eutectic state of the mixture. The melting and crystallization temperatures of CMS ternary eutectic mixture were 23.6 °C and 13.1 °C, and corresponding enthalpies of melting/crystallization were 122.8 kJ/kg and 119.7 kJ/kg, respectively. The phase transition temperatures of prepared CMS ternary eutectic mixture were much lower than those of individual fatty acids, while it still had high values of enthalpy. In addition, the CMS ternary eutectic mixture exhibited desired phase transition temperatures and neared ambient temperature and/or human comfort temperature, which making the CMS ternary eutectic mixture promising for potential applications such as building heating/cooling, indoor temperature controlling, and thermo-regulating fibers and textiles.

DSC curves of CMS ternary eutectic mixture, CMS/CA and CMS/CA-SiO_2 form-stable PCMs are shown in Fig. 10, and the thermal behaviors are summarized in Table 3. The enthalpies of melting/crystallization (both ΔH_m and ΔH_c) of form-stable PCMs were slightly lower than those of the corresponding CMS ternary eutectic mixture, whereas there were no appreciable changes on the phase transition temperatures. Additionally, the results in Table 3 also showed that the ΔH_m and ΔH_c values of form-stable PCMs made of CA-SiO_2 phase inversion membrane were higher than those of form-stable PCMs made of CA phase inversion membrane. As explained previously, the addition of SiO_2 nanoparticles increased surface roughness and specific surface area of phase inversion membrane, leading to the increase of CMS incorporation capability. In other words, the form-stable PCMs made of CA-SiO_2 phase inversion membrane had higher mass fractions of CMS ternary eutectic mixture. It was observed that the resultant form-stable PCMs demonstrated high melting/crystallization heat for thermal storage/retrieval. It is also noteworthy that the heat enthalpies of melting/crystallization of fabricated form-stable PCMs are as high as comparable with those of the phase change composites prepared by physical absorption of

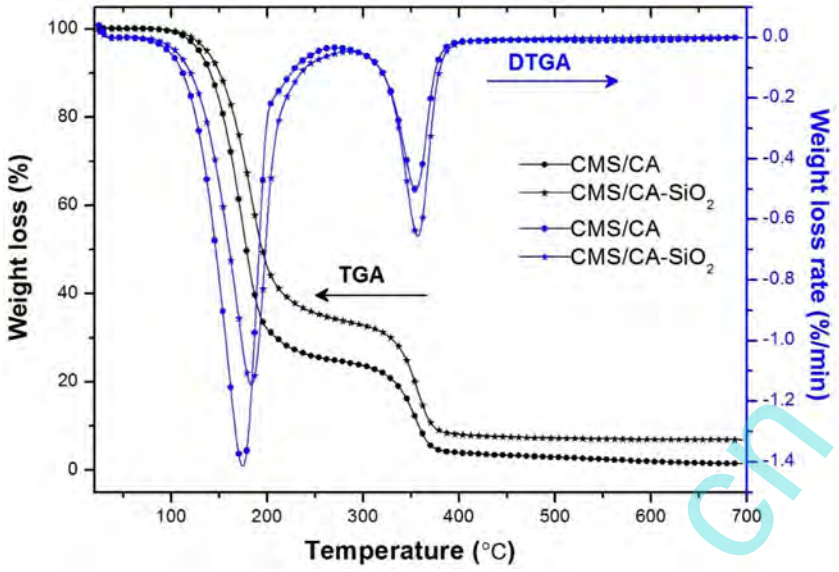

Fig. 11. TGA curves of CMS/CA and CMS/CA-SiO_2 form-stable PCMs.

Table 5
Characteristic temperatures and charred residue at 700 °C of CMS/CA and CMS/CA-SiO_2 form-stable PCMs.

Samples	$T_{-5wt\%}$ (°C)	T_{max1} (°C)	T_{max2} (°C)	Charred residue (%)
CMS/CA	129.5	174.7	354.8	1.5
CMS/CA-SiO_2	137.7	183.8	357.1	6.9

different porous materials with different PCMs (summarized in Table 4). Therefore, the fabricated form-stable PCMs possess high thermal storage capacity and are suitable in the application for thermal energy storage.

3.5. Thermal stability property of form-stable PCMs

Thermal stability property of fabricated form-stable PCMs was evaluated using TGA in N_2 atmosphere. The TGA and DTGA curves of CMS/CA and CMS/CA-SiO_2 form-stable PCMs are shown in Fig. 11, and the 5% weight loss temperature ($T_{-5wt.\%}$), maximum weight loss temperature (T_{max}) and the charred residue at 700 °C are presented in Table 5. It could be found from that there were two steps of degradation process for form-stable PCMs. The first step of degradation occurred roughly from 100 to 240 °C and corresponded to the degradation of the CMS in form-stable PCMs. The second step happened from about 300–400 °C; such a weight loss was attributed to the decomposition of CA in form-stable PCMs. The onset degradation temperature ($T_{-5\ wt.\%}$) for the CMS/CA-SiO_2 form-stable PCMs increased from ~129.5 °C for CMS/CA form-stable PCMs to ~137.7 °C. The maximum weight loss temperature (T_{max1} and T_{max2}) for CMS/CA-SiO_2 form-stable PCMs increased from ~174.7 °C and ~354.8 °C for CMS/CA form-stable PCMs to ~183.8 °C and ~357.1 °C, respectively. The degradation temperature was shifted to higher temperature with addition of SiO_2 nanoparticles. It was also found from Table 5 that the charred residue at 700 °C for CMS/CA-SiO_2 form-stable PCMs was about 6.9 wt.%, and was higher than that of CMS/CA form-stable PCMs (1.5 wt.%). These increases indicated that thermal stability of the CMS/CA-SiO_2 form-stable PCMs was improved, and the improvement was attributed to the SiO_2 nanoparticles. It is known that SiO_2 is an inorganic fire-retardant material, and the SiO_2 nanoparticles on the surface of phase inversion membrane could create a passivation layer during thermal degradation process; additionally, SiO_2 could also act as an insulator and/or mass transport barrier to the volatile byproducts generated during thermal decomposition, leading to the improvement on thermal stability of form-stable PCMs.

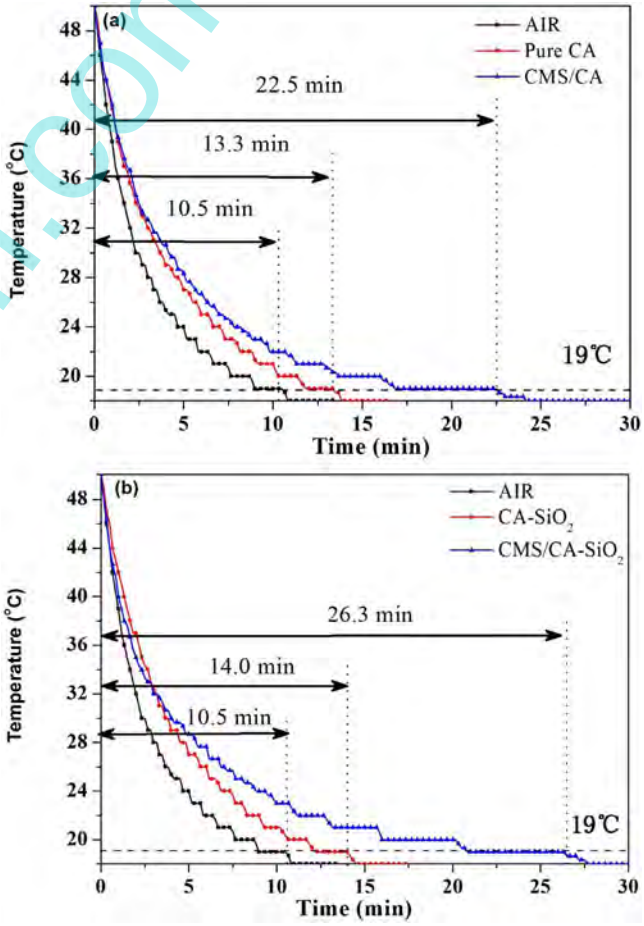

Fig. 12. Curves of thermal performance tests acquired from form-stable PCMs and the corresponding phase inversion membranes: (a) CA and (b) CA-SiO_2.

3.6. Thermal insulation capability of form-stable PCMs

Fig. 12 demonstrates the capability of form-stable PCMs to stabilize

temperature. The thermal insulation capabilities of the CMS/CA and CMS/CA-SiO_2 form-stable PCMs were evaluated by monitoring temperature change of a 50 °C indoor air in a 15 °C environment. For a control sample, *i.e.* without phase inversion membrane, indoor air temperature dropped quickly. It took only ~10.5 min for the control sample to cool from 50 °C down to 19 °C. When the CA phase inversion membrane (without CMS) was placed, indoor air temperature was reduced from 50 °C to 19 °C for ~13.3 min. In contrast, indoor air temperature covered with CMS/CA form-stable PCMs decreased much more slowly. The same temperature change from 50 °C to 19 °C took 22.5 min, as shown in Fig. 12(a). Similar results could also be found for the CMS/CA-SiO_2 form-stable PCMs and the corresponding CA-SiO_2 phase inversion membrane, as shown in Fig. 12(b). The indoor air temperature change from 50 °C to 19 °C took ~14.0 min for CA-SiO_2 phase inversion membrane (without CMS). In comparison with that of CA-SiO_2 phase inversion membrane, the control temperature time for CMS/CA-SiO_2 form-stable PCMs was increased to ~26.3 min. In addition, it could be also observed that the control temperature time of CMS/CA-SiO_2 form-stable PCMs (~26.3 min) was higher than that of CMS/CA form-stable PCMs (~22.5 min), mainly due to CMS/CA-SiO_2 form-stable PCMs with higher CMS ternary eutectic mixture amount. The results indicated that the fabricated form-stable PCMs possessed good thermal insulation capability and temperature regulation ability.

4. Conclusions

In this work, capric-myristic-stearic acid (CMS) ternary eutectic mixture was prepared and incorporated into CA phase inversion membrane to fabricate a novel form-stable PCMs. The addition of SiO_2 nanoparticles into CA phase inversion membrane created porous feature on the resultant CA-SiO_2 phase inversion membrane surface, which facilitated CMS incorporation in the phase inversion membrane. The CA-SiO_2 phase inversion membrane with 10 wt.% SiO_2 amount showed the highest CMS incorporation capacity at ~80.3 wt.%, which due to its high surface roughness and specific surface area. The resultant form-stable PCMs well maintained their structural integrity as well as PCM characteristics. There were two steps of degradation process for form-stable PCMs; and the addition of SiO_2 nanoparticles increased remarkably the onset degradation temperature, maximum weight loss temperature and charred residue of form-stable PCMs, which attributed to improved thermal stability. Compared to the control sample (without phase inversion membrane) and CA-SiO_2 phase inversion membrane, the control temperature times were respectively increased by ~60.1% and 46.8% for the CMS/CA-SiO_2 form-stable PCMs to change its temperature from 50 °C to 19 °C. The fabricated CMS/CA-SiO_2 form-stable PCMs presented good thermal storage/retrieval property and thermal insulation capability, which demonstrated great potential for temperature regulation applications.

Acknowledgements

This research was financially supported by the China Postdoctoral Science Foundation (No. 2015T80496), the Fundamental Research Funds for the Central Universities (No. JUSRP51621A), Jiangsu Universities “Qing Lan” Project (No. 2016 [15]), High-level Innovative and Entrepreneurial Talents in Jiangsu Province (No. 2015 [26]) and the Open Project Program of Key Laboratory of Eco-textiles, Ministry of Education, Jiangnan University (No. KLET1609) .

References

[1] Y.P. Yuan, N. Zhang, W.Q. Tao, X.L. Cao, Y.L. He, Fatty acids as phase change materials: a review, Renew. Sustain. Energy Rev. 29 (2014) 482–498.
[2] S. Harikrishnan, S. Magesh, S. Kalaiselvam, Preparation and thermal energy storage behaviour of stearic acid-TiO_2 nanofluids as a phase change material for solar heating systems, Thermochim. Acta 565 (2013) 137–145.
[3] K. Pielichowska, K. Pielichowski, Phase change materials for thermal energy storage, Prog. Mater. Sci. 65 (2014) 67–123.
[4] M.M. Kenisarin, K.M. Kenisarina, Form-stable phase change materials for thermal energy storage, Renew. Sustain. Energy Rev. 16 (2012) 1999–2040.
[5] L. Cao, D. Su, Y.J. Tang, G.Y. Fang, F. Tang, Properties evaluation and applications of thermal energy storage materials in buildings, Renew. Sustain. Energy Rev. 48 (2015) 500–522.
[6] S. Puupponen, A. Seppala, O. Vartia, K. Saari, T. Ala-Nissila, Preparation of paraffin and fatty acid phase changing nanoemulsions for heat transfer, Thermochim. Acta 601 (2015) 33–38.
[7] D. Wu, B. Ni, Y.J. Liu, S. Chen, H.L. Zhang, Preparation and characterization of side-chain liquid crystal polymer/paraffin composites as form-stable phase change materials, J. Mater. Chem. A 3 (2015) 9645–9657.
[8] X.G. Zhang, Z.H. Huang, B. Ma, R.L. Wen, X. Min, Y.T. Huang, Z.Y. Yin, Y.G. Liu, M.H. Fang, X.W. Wu, Preparation and performance of novel form-stable composite phase change materials based on polyethylene glycol/White Carbon Black assisted by super-ultrasound-assisted, Thermochim. Acta 638 (2016) 35–43.
[9] A. Sharma, A. Shukla, Thermal cycle test of binary mixtures of some fatty acids as phase change materials for building applications, Energy Build. 99 (2015) 196–203.
[10] H. Fauzi, H.S.C. Metselaar, T.M.I. Mahlia, M. Silakhori, Sodium laurate enhancements the thermal properties and thermal conductivity of eutectic fatty acid as phase change material (PCM), Solar Energy 102 (2014) 333–337.
[11] S. Harish, D. Orejon, Y. Takata, M. Kohno, Thermal conductivity enhancement of lauric acid phase change nanocomposite in solid and liquid state with single-walled carbon nanohorn inclusions, Thermochim. Acta 600 (2015) 1–6.
[12] P. Zhang, Q.Y. Yue, H.T. He, B.Y. Gao, Y. Wang, Q. Li, Study on phase diagram of fatty acids mixtures to determine eutectic temperatures and the corresponding mixing proportions, Appl. Energy 115 (2014) 483–490.
[13] H.T. He, P. Zhao, Q.Y. Yue, B.Y. Gao, D.T. Yue, Q. Li, A novel polynary fatty acid/sludge ceramsite composite phase change materials and its applications in building energy conservation, Renew. Energy 76 (2015) 45–52.
[14] L. Cao, Y.J. Tang, G.Y. Fang, Preparation and properties of shape-stabilized phase change materials based on fatty acid eutectics and cellulose composites for thermal energy storage, Energy 80 (2015) 98–103.
[15] Y.B. Cai, M.M. Liu, X.F. Song, J. Zhang, Q.F. Wei, L.F. Zhang, A form-stable phase change material made with a cellulose acetate nanofibrous mat from bicomponent electrospinning and incorporated capric-myristic-stearic acid ternary eutectic mixture for thermal energy storage/retrieval, RSC Adv. 5 (2015) 84245–84251.
[16] X. Zong, Y.B. Cai, G.Y. Sun, Y. Zhao, F.L. Huang, L. Song, Y. Hu, H. Fong, Q.F. Wei, Fabrication and characterization of electrospun SiO_2 nanofibers absorbed with fatty acid eutectics for thermal energy storage/retrieval, Solar Energy Mater. Solar Cells 132 (2015) 183–190.
[17] Y. Wang, T.D. Xia, H.X. Feng, H. Zhang, Stearic acid/polymethyl methacrylate composite as form-stable phase change materials for latent heat thermal energy storage, Renew. Energy 36 (2011) 1814–1820.
[18] L.J. Wang, D. Meng, Fatty acid eutectic/polymethyl methacrylate composite as form-stable phase change material for thermal energy storage, Appl. Energy 87 (2010) 2660–2665.
[19] G.Y. Fang, H. Li, X. Liu, Preparation and properties of lauric acid/silicon dioxide composites as form-stable phase change materials for thermal energy storage, Mater. Chem. Phys. 122 (2010) 533–536.
[20] G.Y. Fang, H. Li, Z. Chen, X. Liu, Preparation and properties of palmitic acid/SiO_2 composites with flame retardant as thermal energy storage materials, Solar Energy Mater. Solar Cells 95 (2011) 1875–1881.
[21] S. Ince, Y. Seki, M.A. Ezan, A. Turgut, A. Erek, Thermal properties of myristic acid/graphite nanoplates composite phase change materials, Renew. Energy 75 (2015) 243–248.
[22] X.J. Yang, Y.P. Yuan, N. Zhang, X.L. Cao, C. Liu, Preparation and properties of myristic-palmitic-stearic acid/expanded graphite composites as phase change materials for energy storage, Solar Energy 99 (2014) 259–266.
[23] X.H. Tang, B. Zhu, M.H. Xu, W. Zhang, Z. Yang, Y.F. Zhang, G.L. Yin, D.N. He, H. Wei, X.Q. Zhai, Shape-stabilized phase change materials based on fatty acid eutectics/expanded graphite composites for thermal storage, Energy Build. 109 (2015) 353–360.
[24] N. Zhang, Y.P. Yuan, Y.X. Du, X.L. Cao, Y.G. Yuan, Preparation and properties of palmitic-stearic acid eutectic mixture/expanded graphite composite as phase change material for energy storage, Energy 78 (2014) 950–956.
[25] Y.G. Yuan, Y.P. Yuan, N. Zhang, Y.X. Du, X.L. Cao, Preparation and thermal characterization of capric-myristic-palmitic acid/expanded graphite composite as phase change material for energy storage, Mater. Lett. 125 (2014) 154–157.
[26] F. Tang, D. Su, Y.J. Tang, G.Y. Fang, Synthesis and thermal properties of fatty acid eutectics and diatomite composites as shape-stabilized phase change materials with enhanced thermal conductivity, Solar Energy Mater. Solar Cells 141 (2015) 218–224.
[27] X.W. Fu, Z.M. Liu, Y. Xiao, J.L. Wang, J.X. Lei, Preparation and properties of lauric acid/diatomite composites as novel form-stable phase change materials for thermal energy storage, Energy Build. 104 (2015) 244–249.
[28] M. Li, H.T. Kao, Z.S. Wu, J.M. Tan, Study on preparation and thermal property of binary fatty acid and the binary fatty acids/diatomite composite phase change materials, Appl. Energy 88 (2011) 1606–1612.
[29] M. Mehrali, S.T. Latibari, M. Mehrali, T.M.I. Mahlia, H.S.C. Metselaar, Effect of carbon nanospheres on shape stabilization and thermal behavior of phase change materials for thermal energy storage, Energy Convers. Manage. 88 (2014) 206–213.
[30] S.K. Song, L.J. Dong, S. Chen, H.A. Xie, C.X. Xiong, Stearic-capric acid eutectic/activated-attapulgiate composite as form-stable phase change material for thermal energy storage, Energy Convers. Manage. 81 (2014) 306–311.
[31] W.D. Liang, P.S. Chen, H.X. Sun, Z.Q. Zhu, A. Li, Innovative spongy attapulgite

loaded with n-carboxylic acids as composite phase change materials for thermal energy storage, RSC Adv. 4 (2014) 38535–38541.
[32] A. Karaipekli, A. Sari, Capric-myristic acid/expanded perlite composite as form-stable phase change material for latent heat thermal energy storage, Renew. Energy 33 (2008) 2599–2605.
[33] N. Zhang, Y.P. Yuan, Y.G. Yuan, T.Y. Li, X.L. Cao, Lauric-palmitic-stearic acid/expanded perlite composite as form-stable phase change material: preparation and thermal properties, Energy Build. 82 (2014) 505–511.
[34] C.M. Jiao, B.H. Ji, D. Fang, Preparation and properties of lauric acid-stearic acid/expanded perlite composite as phase change materials for thermal energy storage, Mater. Lett. 67 (2012) 352–354.
[35] J.S. Liu, Y.Y. Yu, X. He, Research on the preparation and properties of lauric acid/expanded perlite phase change materials, Energy Build. 110 (2016) 108–111.
[36] A. Karaipekli, A. Sari, Preparation, thermal properties and thermal reliability of eutectic mixtures of fatty acids/expanded vermiculite as novel form-stable composites for energy storage, J. Ind. Eng. Chem. 16 (2010) 767–773.
[37] A. Karaipekli, A. Sari, Capric-myristic acid/vermiculite composite as form-stable phase change material for thermal energy storage, Solar Energy 83 (2009) 323–332.
[38] Y.B. Cai, H.Z. Ke, J. Dong, Q.F. Wei, J.L. Lin, Y. Zhao, L. Song, Y. Hu, F.L. Huang, W.D. Gao, H. Fong, Effects of nano-SiO_2 on morphology, thermal energy storage, thermal stability, and combustion properties of electrospun lauric acid/PET ultrafine composite fibers as form-stable phase change materials, Appl. Energy 88 (2011) 2106–2112.
[39] C.Z. Chen, L.G. Wang, Y. Huang, Morphology and thermal properties of electrospun fatty acids/polyethylene terephthalate composite fibers as novel form-stable phase change materials, Solar Energy Mater. Solar Cells 92 (2008) 1382–1387.
[40] Y.B. Cai, C.T. Gao, X.L. Xu, Z. Fu, X.Z. Fei, Y. Zhao, Q. Chen, X.Z. Liu, Q.F. Wei, G.F. He, H. Fong, Electrospun ultrafine composite fibers consisting of lauric acid and polyamide 6 as form-stable phase change materials for storage and retrieval of solar thermal energy, Solar Energy Mater. Solar Cells 103 (2012) 53–61.
[41] Y.B. Cai, C.T. Gao, T. Zhang, Z. Zhang, Q.F. Wei, J.M. Du, Y. Hu, L. Song, Influences of expanded graphite on structural morphology and thermal performance of composite phase change materials consisting of fatty acid eutectics and electrospun PA6 nanofibrous mats, Renew. Energy 57 (2013) 163–170.
[42] Y.B. Cai, X.L. Xu, C.T. Gao, T.Y. Bian, H. Qiao, Q.F. Wei, Structural morphology and thermal performance of composite phase change materials consisting of capric acid series fatty acid eutectics and electrospun polyamide6 nanofibers for thermal energy storage, Mater. Lett. 89 (2012) 43–46.
[43] Y.B. Cai, X. Zong, J.J. Zhang, Y.Y. Hu, Q.F. Wei, G.F. He, X.X. Wang, Y. Zhao, H. Fong, Electrospun nanofibrous mats absorbed with fatty acid eutectics as an innovative type of form-stable phase change materials for storage and retrieval of thermal energy, Solar Energy Mater. Solar Cells 109 (2013) 160–168.
[44] Y.B. Cai, G.Y. Sun, M.M. Liu, J. Zhang, Q.Q. Wang, Q.F. Wei, Fabrication and characterization of capric-lauric-palmitic acid/electrospun SiO_2 nanofibers composite as form-stable phase change material for thermal energy storage/retrieval, Solar Energy 118 (2015) 87–95.
[45] X. Zong, Y.B. Cai, G.Y. Sun, Y. Zhao, F.L. Huang, L. Song, Y. Hu, H. Fong, Q.F. Wei, Fabrication and characterization of electrospun SiO_2 nanofibers absorbed with fatty acid eutectics for thermal energy storage/retrieval, Solar Energy Mater. Solar Cells 132 (2015) 183–190.
[46] Y.B. Cai, M.M. Liu, X.F. Song, J. Zhang, Q.F. Wei, L.F. Zhang, A form-stable phase change material made with a cellulose acetate nanofibrous mat from bicomponent electrospinning and incorporated capric-myristic-stearic acid ternary eutectic mixture for thermal energy storage/retrieval, RSC Adv. 5 (2015) 84245–84251.
[47] D.Y. Xing, N. Peng, T.S. Chung, Formation of cellulose acetate membranes via phase inversion using ionic liquid, BMIM SCN, as the solvent, Ind. Eng. Chem. Res. 49 (2010) 8761–8769.
[48] T. Mohammadi, E. Saljoughi, Effect of production conditions on morphology and permeability of asymmetric cellulose acetate membranes, Desalination 243 (2009) 1–7.
[49] A. Ahmad, S. Waheed, S.M. Khan, S. E-Gul, M. Shafiq, M. Farooq, K. Sanaullah, T. Jamil, Effect of silica on the properties of cellulose acetate/polyethylene glycol membranes for reverse osmosis, Desalination 355 (2015) 1–10.
[50] N. Niksefat, M. Jahanshahi, A. Rahimpour, The effect of SiO_2 nanoparticles on morphology and performance of thin film composite membranes for forward osmosis application, Desalination 343 (2014) 140–146.
[51] J. Yin, E.S. Kim, J. Yang, B. Deng, Fabrication of a novel thin-film nanocomposite (TFN) membrane containing MCM-41 silica nanoparticles (NPs) for water purification, J. Membr. Sci. 423 (2012) 238–246.
[52] G. Arthanareeswaran, T.K.S. Devi, M. Raajenthiren, Effect of silica particles on cellulose acetate blend ultrafiltration membranes: part I, Sep. Purif. Technol. 68 (2008) 38–47.
[53] J. Dasgupta, S. Chakraborty, J. Sikder, R. Kumar, D. Pal, S. Curcio, E. Drioli, The effects of thermally stable titanium silicon oxide nanoparticles on structure and performance of cellulose acetate ultrafiltration membranes, Sep. Purif. Technol. 133 (2014) 55–68.
[54] Y.J. Wang, L.R. Yang, G.S. Luo, Y.Y. Dai, Preparation of cellulose acetate membrane filled with metal oxide particles for the pervaporation separation of methanol/methyl tert-butyl ether mixtures, Chem. Eng. J. 146 (2009) 6–10.